Modelling and Analysis of Non-Stationary Multipath Fading Channels with Time-Variant Angles of Arrival

Matthias Pätzold
University of Agder
Faculty of Engineering and Science
NO-4898 Grimstad, Norway
Email: matthias.paetzold@uia.no

Carlos A. Gutierrez
Universidad Autonoma de San Luis
San Luis Potosi 78290, Mexico
Email: cagutierrez@ieee.org

***Abstract*—In mobile radio channel modelling, it is generally assumed that the angles of arrival (AOAs) are independent of time. This assumption does in general not agree with real-world channels in which the AOAs vary with the position of a moving receiver. In this paper, we first present a mathematical model for the time-variant AOAs. This model serves as the basis for the development of two non-stationary multipath fading channels models. The statistical properties of both channel models are analysed with emphasis on the time-dependent autocorrelation function (ACF), time-dependent mean Doppler shift, time-dependent Doppler spread, and the Wigner-Ville spectrum. It is shown that these characteristic quantities are greatly influenced by time-variant AOAs. The presented analytical framework provides a new view on the channel characteristics that goes well beyond ultra-short observation intervals over which the channel can be considered as wide-sense stationary.**

I. Introduction

In a typical downlink scenario, where plane waves travel from a base station (BS) to a mobile station (MS) via a large number of fixed scattering objects, the angles of arrival (AOAs) of the received signals are changing along the moving route of the MS. Only for very short observation intervals in which the MS travels a few tens of the wavelength [1], the temporal variation of the AOAs can be neglected justifying the wide-sense stationary assumption of multipath fading channels. The lengths of the stationary intervals during which the mobile radio channel can be considered as wide-sense stationary or quasi-stationary has been investigated, e.g., in [2]–[4] and in the references therein. By pushing the observation interval beyond the stationary interval, the received signal captures non-stationary effects that call for new channel modelling approaches using time-frequency analysis techniques [5]. One of the effects that comes with long observation intervalls is that the AOAs are changing with time.

Attempts to include the temporal variations of the AOAs in mobile radio channel models have been made in [6]–[8]. In [6], a non-stationary multiple-input multiple-output (MIMO) vehicle-to-vehicle channel model has been derived by assuming that the AOAs and AODs are piecewise constant. In [7], a proposal has been made for the extension of the IMT-Advanced channel model [9] by replacing the time-invariant model parameters, such as the propagation delays, AOAs, and the angels of departure (AODs) by time-variant parameters. In [8], a non-stationary one-ring model has been introduced in which the time-variant AOAs have been modelled by stochastic processes rather than random variables.

This paper expands on the recent results by studying the impact of time-variant AOAs on the statistical properties of multipath fading channels. It is shown that the multipath fading channel becomes non-wide-sense stationary if the AOAs change with time. Two new non-stationary channel models with time-variant AOAs are derived. The first one has an instantaneous channel phase that is related to the instantaneous Doppler frequency via the phase-frequency relationship [10], while the second one is based on a Taylor series approximation of the instantaneous channel phase. This approximation results in a simpler but less accurate non-stationary channel model that can be identified as a sum-of cisoids (SOC) model in which the Doppler frequencies are varying with time. The statistical properties of both channel models are investigated with emphasis on the time-dependent autocorrelation function (ACF), time-dependent mean Doppler shift, time-dependent Doppler spread, and the Wigner-Ville spectrum. Our analysis shows that our first proposed non-stationary channel model is consistent w.r.t. the mean Doppler shift and the Doppler spread, while this consistency property is not fulfilled by the SOC model with time-variant Doppler frequencies. The two proposed non-stationary channel models provide a trade-off between accuracy and complexity concerning the mathematical expressions.

The organization of this paper is as follows. Section II presents the derivation of two non-stationary multipath fading channel models. Their statistical properties will be analysed in Section III. The numerical key results of our study are visualized in Section IV. Finally, Section V draws the conclusion and suggests possible future research topics in relation to the issues addressed in this paper.

DOI 10.1109/VTCSpring.2017.8108201

II. Derivation of the Non-Stationary Multipath Channel Models

A. Time-Variant AOAs

We consider a downlink non-line-of-sight (NLOS) propagation scenario in which a fixed BS operates as transmitter, and an MS acts as receiver. It is supposed that the BS and the MS are equipped with omnidirectional antennas. The BS antenna is elevated and unobstructed by any object, whereas the MS antenna is surrounded by a large number of N fixed scattering objects called henceforth scatterers S_n $(n = 1, 2, \ldots, N)$. The coordinate system has been chosen such that the MS is located at the origin $(0, 0)$ of the xy-plane at $t = 0$. Furthermore, it is assumed that the MS moves with constant velocity $\vec{\mathrm{v}}$ in the direction determined by the angle of motion α_{v} as indicated in Fig. 1. For reasons of clarity, this figure

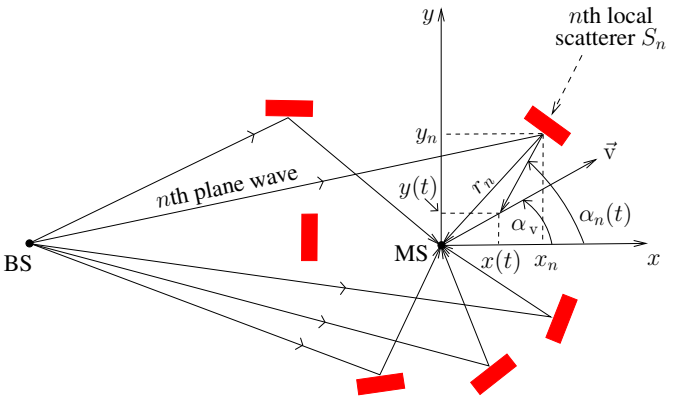

Fig. 1: A multipath propagation scenario with time-variant AOAs $\alpha_n(t)$.

highlights only the location of the scatterer S_n from which the MS receives the nth multipath component (plane wave) $\mu_n(t)$ in the form of $\mu_n(t) = c_n \exp\{j\theta_n(t)\}$, where c_n denotes the path gain which is supposed to be constant, and $\theta_n(t)$ is the associated channel phase that will be studied in Section II-C. The corresponding AOA $\alpha_n(t)$ is defined as the angle between the propagation direction of the nth incident plane wave and the x-axis, i.e.,

$$\alpha_n(t) = \arctan\left(\frac{y_n - y(t)}{x_n - x(t)}\right) \tag{1}$$

for $n = 1, 2, \ldots, N$, where x_n and y_n denote the coordinates of the scatterer S_n; and $x(t)$ and $y(t)$ indicate the position of the MS at time t. According to (1), the AOA $\alpha_n(t)$ is a nonlinear function of time t, which can be turned into a linear function by developing $\alpha_n(t)$ in a Taylor series around $t = 0$ and retaining only the first two terms. This results in the following model for the time-variant AOA

$$\alpha_n(t) = \alpha_n + \gamma_n \cdot t \tag{2}$$

where

$$\alpha_n = \alpha_n(0) = \arctan\left(\frac{y_n}{x_n}\right) \tag{3}$$

$$\gamma_n = \frac{d}{dt}\alpha_n(t)\bigg|_{t=0} = \frac{\mathrm{v}}{r_n}\sin(\alpha_n - \alpha_{\mathrm{v}})\,. \tag{4}$$

In (4), r_n denotes the distance from the scatterer S_n to the origin of the xy-plane, i.e., $r_n = \sqrt{x_n^2 + y_n^2}$, as can be deduced from the geometrical model in Fig. 1. In Section IV, it is shown that the two-term Taylor series expansion of $\alpha_n(t)$ in (2) is sufficiently accurate for small observation intervals T.

B. Time-Variant Doppler Frequencies

Owing to the Doppler effect combined with the new feature that the AOAs $\alpha_n(t)$ vary with time, it follows that the nth incident plane wave highlighted in Fig. 1 experiences a time-variant Doppler shift of $f_n(t) = f_{\max}\cos(\alpha_n(t) - \alpha_{\mathrm{v}})$ that can be expressed by using (2) as

$$f_n(t) = f_{\max}\cos(\alpha_n - \alpha_{\mathrm{v}} + \gamma_n t) \tag{5}$$

for $n = 1, 2, \ldots, N$, where $f_{\max}$ stands for the maximum Doppler frequency. For a given propagation scenario with constant parameters $f_{\max}, \alpha_n, \alpha_{\mathrm{v}}$, and γ_n, the time-variant Doppler shift $f_n(t)$ is a deterministic function of time. Otherwise, if one or several model parameters, e.g., α_n, and thus γ_n, are random variables, then $f_n(t)$ represents a stochastic process. If the MS moves during the time interval $[0, T]$, then $f_n(t)$ describes a curve starting from the initial Doppler frequency $f_n(0) = f_{\max}\cos(\alpha_n - \alpha_{\mathrm{v}})$ and ending with the finishing Doppler frequency $f_n(T) = f_{\max}\cos(\alpha_n - \alpha_{\mathrm{v}} + \gamma_n T)$.

The time-variant Doppler shift $B_f^{(1)}(t)$ and the time-variant Doppler spread $B_f^{(2)}(t)$ can be computed according to

$$B_f^{(1)}(t) = \frac{\sum\limits_{n=1}^{N} c_n^2 f_n(t)}{\sum\limits_{n=1}^{N} c_n^2} \tag{6}$$

and

$$B_f^{(2)}(t) = \sqrt{\frac{\sum\limits_{n=1}^{N} c_n^2 f_n^2(t)}{\sum\limits_{n=1}^{N} c_n^2} - \left(B_f^{(1)}(t)\right)^2}\,. \tag{7}$$

C. Instantaneous Channel Phase

The instantaneous channel phase $\theta_n(t)$ of the nth multipath component $\mu_n(t) = c_n \exp\{j\theta_n(t)\}$ is related to the instantaneous Doppler frequency $f_n(t)$ via the phase-frequency relationship [5, Eq. (1.3.40)]

$$\theta_n(t) = 2\pi \int_{-\infty}^{t} f_n(x)\, dx \tag{8}$$

for $n = 1, 2, \ldots, N$. Using (5), the instantaneous phase $\theta_n(t)$ can be developed as follows:

$$\begin{aligned}\theta_n(t) &= \underbrace{2\pi \int_{-\infty}^{0} f_n(x)\,dx}_{\theta_n} + 2\pi \int_{0}^{t} f_n(x)\,dx \\ &= \theta_n + 2\pi \frac{f_{\max}}{\gamma_n} \left[\sin(\alpha_n - \alpha_{\rm v} + \gamma_n t) - \sin(\alpha_n - \alpha_{\rm v})\right]\end{aligned} \tag{9}$$

where $\theta_n = \theta_n(0)$ denotes the initial phase at $t = 0$. The phases θ_n are generally unknown and modelled by independent identically distributed (i.i.d.) random variables, each with uniform distribution over the interval $(0, 2\pi]$, i.e., $\theta_n \sim \mathcal{U}(0, 2\pi]$. Equation (9) tells us that the instantaneous phase $\theta_n(t)$ is not only a non-linear function of time t but also periodic with period $T_n = 2\pi/\gamma_n$ if the AOA $\alpha_n(t)$ varies with time according to (2). In the limit $\gamma_n \to 0$, however, it can be shown by applying L'Hôpital's rule to (9) that

$$\lim_{\gamma_n \to 0} \theta_n(t) = \theta_n + 2\pi f_n t \tag{10}$$

where $f_n = f_n(0) = f_{\max} \cos(\alpha_n - \alpha_{\rm v})$. This result reveals a linear relationship between the instantaneous phase $\theta_n(t)$ and time t, which holds only for constant AOAs $\alpha_n(t) = \alpha_n$. It should be noticed that the expression in (10) can be identified as the standard phase term of SOC channel models for Rayleigh/Rice fading channels [11, Section 4.5].

A simpler but less accurate expression than (9) can be obtained for the instantaneous phase $\theta_n(t)$ by developing $\theta_n(t)$ in a second-order Taylor series around $t = 0$ as follows:

$$\begin{aligned}\alpha_n(t) &\approx \theta_n(0) + \theta_n'(0)t \\ &= \theta_n + 2\pi f_{\max} \cos(\alpha_n - \alpha_{\rm v} + \gamma_n t)t \\ &= \theta_n + 2\pi f_n(t)t\end{aligned} \tag{11}$$

where $\theta_n'(0)$ denotes the time derivative of $\theta_n(t)$ at $t = 0$. By comparing the last two equations, we can conclude that the non-linear phase term $\theta_n(t)$ in (11) can be obtained from the standard phase term $\theta_n(t)$ in (10) by substituting the instantaneous Doppler frequencies $f_n(t)$ for the time-independent Doppler frequencies f_n. This intuitive mathematical manipulation results in a non-stationary channel model that is inconsistent w.r.t. the mean Doppler shift $B_f^{(1)}(t)$ and the Doppler spread $B_f^{(2)}(t)$, as we will see in Section III-B.

D. Complex Channel Gain

A model for the complex channel gain, denoted by $\mu(t)$, of a narrowband multipath fading channel is obtained by the superposition of all N plane wave components $\mu_n(t) = c_n \exp\{j\theta_n(t)\}$, i.e.,

$$\mu(t) = \sum_{n=1}^{N} c_n e^{\,j\theta_n(t)}\,. \tag{12}$$

Substituting the instantaneous channel phase $\theta_n(t)$ according to (9) in (12) results in the complex channel gain of the proposed non-stationary multipath fading channel with time-variant AOAs

$$\mu(t) = \sum_{n=1}^{N} c_n e^{\,j\{2\pi \frac{f_{\max}}{\gamma_n}[\sin(\alpha_n - \alpha_{\rm v} + \gamma_n t) - \sin(\alpha_n - \alpha_{\rm v})] + \theta_n\}}\,. \tag{13}$$

On the other hand, if we substitute the approximation (11) in (12), then we obtain the complex channel gains $\mu(t)$ in a much simpler form, namely

$$\mu(t) = \sum_{n=1}^{N} c_n e^{\,j(2\pi f_n(t)\cdot t + \theta_n)}\,. \tag{14}$$

From the discussions in the previous subsection, it can be summed up that the two complex channel gains $\mu(t)$ in (13) and (14) include the SOC model [12]

$$\mu(t) = \sum_{n=1}^{N} c_n e^{\,j(2\pi f_n t + \theta_n)} \tag{15}$$

as a special case that arises if the AOA $\alpha_n(t)$ is supposed to be constant ($\gamma_n = 0$). The main difference between the three stochastic channel models above is that the former two are non-wide-sense stationary, whereas the third one is wide-sense stationary. The statistical properties of the SOC model have been studied in [12], while those of the new non-wide-sense stationary models will be analysed in the next section.

III. Analysis of the Non-Stationary Multipath Channel Models

A. Time-Dependent ACF

The time-dependent ACF $\mathcal{R}_\mu(\tau, t)$ of a complex stochastic process $\mu(t)$ is defined as

$$\mathcal{R}_\mu(\tau, t) = E\left\{\mu\left(t + \frac{\tau}{2}\right)\mu^*\left(t - \frac{\tau}{2}\right)\right\} \tag{16}$$

where $E\{\cdot\}$ denotes the expectation operator and $(\cdot)^*$ stands for the complex conjugation operator. In Appendix A, it is proved that the time-dependent ACF $\mathcal{R}_\mu(\tau, t)$ of the complex channel gain $\mu(t)$ described by (13) can be written as

$$\mathcal{R}_\mu(\tau, t) = \sum_{n=1}^{N} c_n^2 e^{\,j2\pi f_n(t)\cdot \mathrm{sinc}(\gamma_n \tau/2)\cdot \tau} \tag{17}$$

where $\mathrm{sinc}(\cdot)$ denotes the sinc function, which is defined by $\mathrm{sinc}(x) = \sin(x)/x$.

Analogously, it can be shown that the time-dependent ACF $\mathcal{R}_\mu(\tau, t)$ of the complex channel gain $\mu(t)$ introduced in (14) can be expressed by

$$\mathcal{R}_\mu(\tau, t) = \sum_{n=1}^{N} c_n^2\, e^{\,j2\pi[f_n(t)\cos(\gamma_n \frac{\tau}{2}) + f_n'(t)\mathrm{sinc}(\gamma_n \frac{\tau}{2})t]\tau} \tag{18}$$

where $f_n(t)$ is the time-variant Doppler shift in (5) and $f_n'(t)$ denotes its derivative w.r.t. time t.

For the special case that the AOA $\alpha_n(t)$ is constant, i.e., $\gamma_n = 0$, it is obvious that the two time-dependent ACFs in (17) and (18) reduce to

$$\mathcal{R}_\mu(\tau) = \mathcal{R}_\mu(\tau, t) = \sum_{n=1}^{N} c_n^2 \, e^{\,j2\pi f_n \tau} \tag{19}$$

which represents the ACF of the SOC model described by (15). In this case, the ACF depends only on the time separation τ but not on the time t, which was to be expected, because the SOC process $\mu(t)$ is wide-sense stationary.

Furthermore, if $\gamma_n = 0$ and $\alpha_n \sim \mathcal{U}(0, 2\pi]$, then the expressions in (17)–(19) reduce to the ACF $\mathcal{R}_\mu(\tau) = 2\sigma_0^2 J_0(2\pi f_{\max}\tau)$, where $2\sigma_0^2 = \sum_{n=1}^{N} c_n^2$ denotes the mean power of the complex channel gain $\mu(t)$, and $J_0(\cdot)$ is the zeroth-order Bessel function of the first kind [13, Eq. (8.411-1)]. In other words, the proposed non-stationary multipath fading channel models include the classical Jakes/Clarke model [1], [14] as a special case.

B. Time-Dependent Mean Doppler Shift and Time-Dependent Doppler Spread

From the time-dependent ACF $\mathcal{R}_\mu(\tau, t)$, the time-dependent mean Doppler shift $B_\mu^{(1)}(t)$ and the time-dependent Doppler spread $B_\mu^{(2)}(t)$ can be derived by means of

$$B_\mu^{(1)}(t) = \frac{1}{2\pi j} \frac{\dot{\mathcal{R}}_\mu(0, t)}{\mathcal{R}_\mu(0, t)} \tag{20}$$

and

$$B_\mu^{(2)}(t) = \frac{1}{2\pi} \sqrt{\left(\frac{\dot{\mathcal{R}}_\mu(0, t)}{\mathcal{R}_\mu(0, t)}\right)^2 - \frac{\ddot{\mathcal{R}}_\mu(0, t)}{\mathcal{R}_\mu(0, t)}} \tag{21}$$

respectively, where $\dot{\mathcal{R}}_\mu(0, t)$ ($\ddot{\mathcal{R}}_\mu(0, t)$) denotes the first (second) order derivative of $\mathcal{R}_\mu(\tau, t)$ w.r.t. τ at $\tau = 0$. Inserting (17) in (20) and (21) results after some straightforward mathematical steps in the following closed-form solutions

$$B_\mu^{(1)}(t) = \frac{\sum\limits_{n=1}^{N} c_n^2 f_n(t)}{\sum\limits_{n=1}^{N} c_n^2} \tag{22}$$

$$B_\mu^{(2)}(t) = \sqrt{\frac{\sum\limits_{n=1}^{N} c_n^2 f_n^2(t)}{\sum\limits_{n=1}^{N} c_n^2} - \left(B_\mu^{(1)}(t)\right)^2}. \tag{23}$$

A comparison of (22) with (6) and (23) with (7) reveals that the equalities $B_\mu^{(1)}(t) = B_f^{(1)}(t)$ and $B_\mu^{(2)}(t) = B_f^{(2)}(t)$ hold, from which we can conclude that the proposed non-stationary multipath fading channel model described by (13) is consistent with respect to both the mean Doppler shift and the Doppler spread.

On the other hand, if we insert (18) in (20) and (21), then we obtain

$$B_\mu^{(1)}(t) = \frac{\sum\limits_{n=1}^{N} c_n^2 (f_n(t) + f_n'(t) \cdot t)}{\sum\limits_{n=1}^{N} c_n^2} \tag{24}$$

and

$$B_\mu^{(2)}(t) = \sqrt{\frac{\sum\limits_{n=1}^{N} c_n^2 (f_n(t) + f_n'(t) \cdot t)^2}{\sum\limits_{n=1}^{N} c_n^2} - \left(B_\mu^{(1)}(t)\right)^2}. \tag{25}$$

This result demonstrates that the simple non-stationary channel model introduced in (14) is inconsistent w.r.t. the mean Doppler shift and the Doppler spread, because $B_\mu^{(1)}(t) \neq B_f^{(1)}(t)$ and $B_\mu^{(2)}(t) \neq B_f^{(2)}(t)$ hold. Concerning the SOC process $\mu(t)$ in (15), we mention for completeness that the equalities $B_\mu^{(1)} = B_f^{(1)}$ and $B_\mu^{(2)} = B_f^{(2)}$ hold, where $B_\mu^{(1)}$ and $B_\mu^{(2)}$ are the same quantities as in (22) and (23), respectively, if we replace there $f_n(t)$ by f_n. Thus, the SOC model is consistent w.r.t. the mean Doppler shift and the Doppler spread.

C. Wigner-Ville Spectrum

The Wigner-Ville spectrum[1] $\mathcal{S}_\mu(f, t)$ is defined as the Fourier transform of the time-dependent ACF $\mathcal{R}_\mu(\tau, t)$ w.r.t. τ [10], i.e.,

$$\mathcal{S}_\mu(f, t) = \int_{-\infty}^{\infty} \mathcal{R}_\mu(\tau, t) e^{\,-j2\pi f t} d\tau \,. \tag{26}$$

Inserting (17) in (26) and using the property $\mathcal{R}_\mu(\tau, t) = \mathcal{R}_\mu^*(-\tau, t)$, we can express the Wigner-Ville spectrum $\mathcal{S}_\mu(f, t)$ of the proposed non-stationary multipath fading channel model described by (13) as

$$\mathcal{S}_\mu(f, t) = 2 \sum_{n=1}^{N} c_n^2 \int_0^{\infty} \cos\left\{2\pi \left[f - f_n(t) \mathrm{sinc}\left(\gamma_n \frac{\tau}{2}\right)\right] \tau\right\} d\tau \,. \tag{27}$$

For the wide-sense stationary case, for which $\gamma_n = 0$ holds, the Wigner-Ville spectrum $\mathcal{S}_\mu(f, t)$ in (27) reduces to the Doppler power spectral density (PSD) of the SOC process $\mu(t)$ in (15)

$$\mathcal{S}_\mu(f) = \sum_{n=1}^{N} c_n^2 \, \delta(f - f_n) \,. \tag{28}$$

Furthermore, for the isotropic scattering case, in which c_n and α_n are i.i.d. random variables with $E\{c_n^2\} = 2\sigma_0^2/N$ and $\alpha_n \sim \mathcal{U}(0, 2\pi]$, we obtain the Jakes/Clarke PSD [1], [14] after computing the expected value of $\mathcal{S}_\mu(f)$ in (28). Hence, the Wigner-Ville spectrum $\mathcal{S}_\mu(f, t)$ in (27) includes the classical Jakes/Clarke Doppler spectrum as a special case.

[1]The Wigner-Ville spectrum is also called the time-varying spectrum or the evolutive spectrum.

IV. Numerical Results

This section presents a selection of numerical results to illustrate the main findings of this paper. In all considered propagation scenarios, we have set the number of multipath components N to $N = 10$. The gains c_n and initial AOAs $\alpha_n = \alpha_n(0)$ have been computed by using the extended method of exact Doppler spread (EMEDS) [15]. According to this method, the parameters c_n and α_n are given by

$$c_n = \sigma_0 \sqrt{\frac{2}{N}} \quad \text{and} \quad \alpha_n = \frac{2\pi}{N}\left(n - \frac{1}{4}\right) \tag{29}$$

respectively, and the initial phases $\theta_n = \theta_n(0)$ are considered as realizations of independent random variables, each characterized by a uniform distribution over the interval $(0, 2\pi]$. The radii r_n in Fig. 1 have been set to 50 m for all $n = 1, 2, \ldots, N$. For the mean power (variance) σ_0^2 of the inphase and quadrature components of $\mu(t)$, we have chosen the value $\sigma_0^2 = 1$. The maximum Doppler frequency $f_{\max}$ was supposed to be $f_{\max} = 91\,\text{Hz}$. Furthermore, we have assumed that the MS moves with speed $\text{v} = |\vec{\text{v}}| = 110\,\text{km/h}$ in x-direction, implying that $\alpha_\text{v} = 0$.

Fig. 2 depicts the trend of the time-variant Doppler frequencies $f_n(t)$ by using the exact expression for the AOAs $\alpha_n(t)$ according to (1). For comparison, this figure also shows the behaviour of $f_n(t)$ for the approximate solution of $\alpha_n(t)$ in (2). Fig. 2 shows clearly that the first-order approximation is quite good over the interval from 0 to $T_\text{sim} = 1.64\,\text{s}$.

Fig. 3 illustrates the signal envelope $|\mu(t)|$ by using the SOC model [see (15), Case I], the proposed non-stationary multipath fading channel model [see (13), Case II], and the simple non-stationary model [see (14), Case III]. This figure demonstrates clearly that the temporal variations of the AOAs $\alpha_n(t)$ have a great influence on the characteristics of the signal envelope $|\mu(t)|$.

Figs. 4 and 5 present the ACF $\mathcal{R}_\mu(\tau)$ of the SOC process $\mu(t)$ in (15) and the time-dependent ACF $\mathcal{R}_\mu(\tau, t)$ of the non-stationary process $\mu(t)$ in (13), respectively. It can be observed that both ACFs are identical at the origin $t = 0$, but the temporal correlation properties of the non-stationary model differ more and more if time t proceeds. This means that the temporal variations of $\alpha_n(t)$ influence greatly the fading behaviour of the signal envelope $|\mu(t)|$.

Figs. 6 and 7 depict the corresponding Doppler PSD $\mathcal{S}_\mu(f)$ [see (28)] of the SOC process $\mu(t)$ in (15) and the Wigner-Ville spectrum $\mathcal{S}_\mu(f, t)$ [see (27)] of the non-stationary process $\mu(t)$ in (13), respectively. A comparison of the two spectral representations shows clearly that the influence of the time-variant AOAs $\alpha_n(t)$ cannot be neglected.

V. Conclusion

In this paper, we have developed and analysed multipath fading channel models with time-variant AOAs. Our study has shown that the effect of time-variant AOAs results in a non-wide-sense stationary multipath fading channel model. Expressions have been derived for the time-dependent ACF, time-dependent mean Doppler shift, time-dependent Doppler spread, and the Wigner-Ville spectrum of the proposed non-wide-sense stationary channel model. By comparing these statistical quantities with known results of studies assuming constant AOAs, we can conclude that the assumption of constant AOAs is only justified for very short observation intervals. The proposed non-stationary channel model allows extending the observation interval over a wider range without losing accuracy. The price for this added accuracy is a higher degree of complexity concerning the mathematical expressions.

One of the remaining problems that might be tackled in an upcoming study is to develop quantitative methods for the investigation of the length of the observation interval over which the proposed non-stationary channel models are sufficiently accurate. Another topic could be to extend the presented framework to the modelling of MIMO channels with time-dependent AOAs.

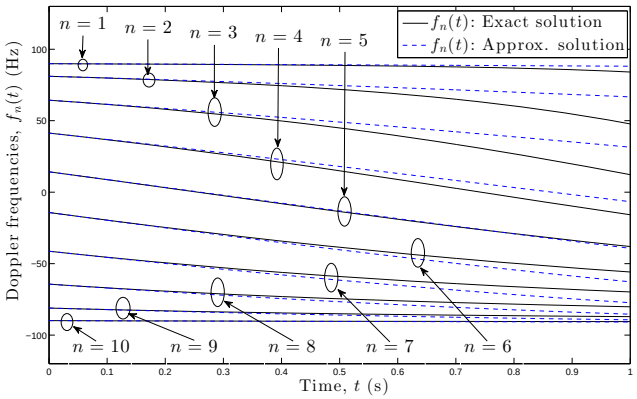

Fig. 2: Trend of the time-variant Doppler frequencies $f_n(t)$ $(n = 1, 2, \ldots, N)$ by using the exact solution (——) and the approximate solution (- - -), where $N = 10$.

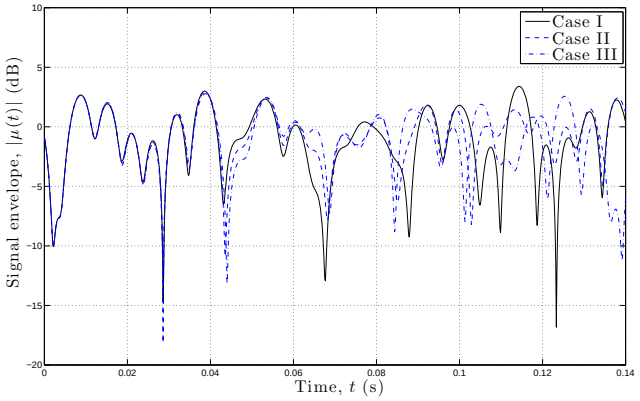

Fig. 3: Illustration of the signal envelope $|\mu(t)|$ of a sample function of a wide-sense stationary SOC process [see (15)] in comparison with the signal envelopes $|\mu(t)|$ of the non-stationary processes described by (13) and (14).

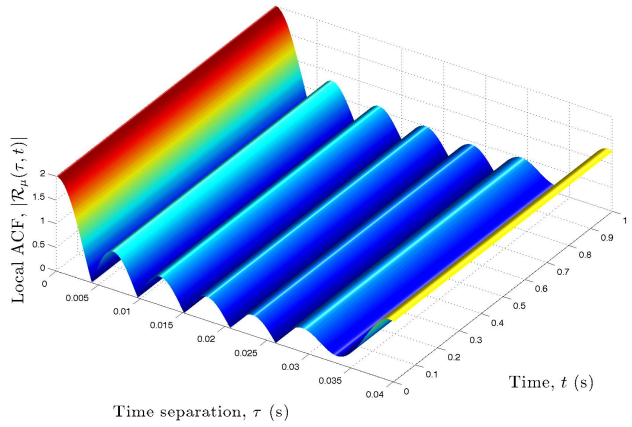

Fig. 4: ACF $\mathcal{R}_\mu(\tau) = \mathcal{R}_\mu(\tau,t)$ of a SOC process $\mu(t)$ with constant AOAs α_n for $N = 10$.

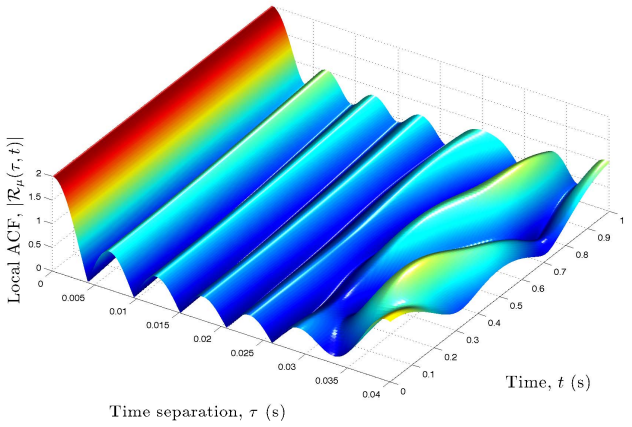

Fig. 5: Time-dependent ACF $\mathcal{R}_\mu(\tau,t)$ of the proposed non-stationary process $\mu(t)$ with time-variant AOAs $\alpha_n(t)$ for $N = 10$.

APPENDIX

A. Derivation of the Time-Dependent ACF $\mathcal{R}_\mu(\tau,t)$ in (17)

Substituting (13) in the definition of the time-dependent ACF $\mathcal{R}_\mu(\tau,t) = E\{\mu(t+\tau/2)\mu^*(t-\tau/2)\}$ gives

$$\mathcal{R}_\mu(\tau,t) = E\left\{\sum_{n=1}^{N}\sum_{n=1}^{N} c_n c_m \, e^{j\{2\pi\frac{f_{\max}}{\gamma_n}[\sin(\alpha_n-\alpha_v+\gamma_n(t+\frac{\tau}{2}))-\sin(\alpha_n-\alpha_v)]+\theta_n\}} \, e^{-j\{2\pi\frac{f_{\max}}{\gamma_m}[\sin(\alpha_m-\alpha_v+\gamma_m(t-\frac{\tau}{2}))-\sin(\alpha_m-\alpha_v)]+\theta_m\}}\right\}. \tag{A.1}$$

Using $E\{e^{j(\theta_n-\theta_m)}\} = 1$ if $n = m$ and 0 if $n \neq m$, we obtain

$$\begin{aligned}\mathcal{R}_\mu(\tau,t) &= \sum_{n=1}^{N} c_n^2 e^{j2\pi\frac{f_{\max}}{\gamma_n}\sin(\alpha_n-\alpha_v+\gamma_n(t+\frac{\tau}{2}))} \cdot e^{-j2\pi\frac{f_{\max}}{\gamma_n}\sin(\alpha_n-\alpha_v+\gamma_n(t-\frac{\tau}{2}))} \\ &= \sum_{n=1}^{N} c_n^2 e^{j2\pi\frac{f_{\max}}{\gamma_n/2}\cos(\alpha_n-\alpha_v+\gamma_n t)\sin(\gamma_n\frac{\tau}{2})} \\ &= \sum_{n=1}^{N} c_n^2 e^{j2\pi f_n(t)\mathrm{sinc}(\gamma_n\tau/2)\tau} \end{aligned} \tag{A.2}$$

where we have used the sinc function defined as $\mathrm{sinc}(x) = \sin(x)/x$.

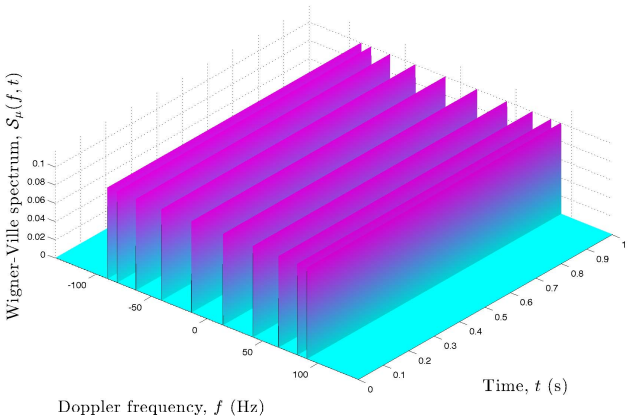

Fig. 6: Wigner-Ville spectrum (Doppler PSD) $\mathcal{S}_\mu(f) = \mathcal{S}_\mu(f,t)$ of an SOC process $\mu(t)$ with constant AOAs α_n for $N = 10$.

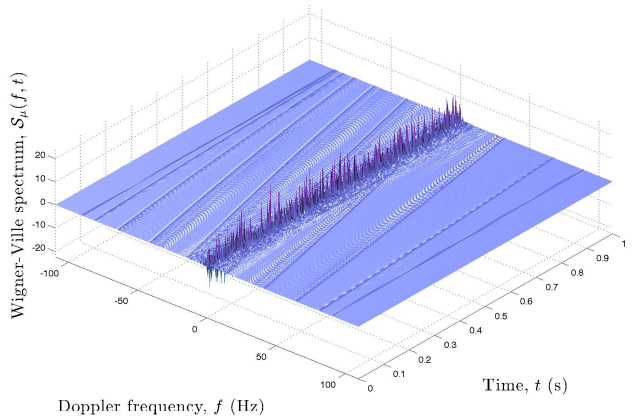

Fig. 7: Wigner-Ville spectrum $\mathcal{S}_\mu(f,t)$ of the proposed non-stationary process $\mu(t)$ with time-variant AOAs $\alpha_n(t)$ for $N = 10$.

REFERENCES

[1] W. C. Jakes, Ed., *Microwave Mobile Communications*. Piscataway, NJ: IEEE Press, 1994.

[2] R. He *et al.*, "Characterization of quasi-stationarity regions for vehicle-to-vehicle radio channels," *IEEE Trans. Antennas Propag.*, vol. 63, no. 5, pp. 2237–2251, May 2015.

[3] D. Umansky and M. Pätzold, "Stationarity test for wireless communication channels," in *Proc. IEEE Global Communications Conference, IEEE GLOBECOM 2009*. Honolulu, Hawaii, USA, Nov./Dec. 2009.

[4] A. Ispas, C. Schneider, G. Ascheid, and R. Thomä, "Analysis of the local quasi-stationarity of measured dual-polarized MIMO channels," *IEEE Trans. Veh. Technol.*, vol. 64, no. 8, pp. 3481–3493, Aug. 2015.

[5] B. Boashash, Ed., *Time-Frequency Signal Analysis and Processing: A Comprehensive Reference*, 2nd ed. Elsevier Academic Press, 2015.

[6] A. Chelli and M. Pätzold, "A non-stationary MIMO vehicle-to-vehicle

channel model based on the geometrical T-junction model," in *Proc. International Conference on Wireless Communications and Signal Processing, WCSP 2009*. Nanjing, China, Nov. 2009.

[7] Z. Zhu, Y. Zhu, T. Zhang, and Z. Zeng, "A time-variant MIMO channel model based on the IMT-Advanced channel model," in *Proc. Int. Conference on Wireless Commun. & Signal Process., WCSP 2012*. Huangshan, China, Oct. 2012.

[8] A. Borhani and M. Pätzold, "A non-stationary one-ring scattering model," in *Proc. IEEE Wireless Communications and Networking Conference, WCNC 2013*. Shanghai, China, Apr. 2013, pp. 2661–2666.

[9] ITU-R Rep. M2135, "Guidelines for evaluation of radio interface technologies for IMT-Advanced," 2008. [Online]. Available: http://www.itu.int/dms_pub/itu-r/opb/rep/R-REP-M.2135-2008-PDF-E.pdf

[10] W. Martin, "Time-frequency analysis of random signals," in *Proc. IEEE Internat. Conf. on Aucoustics, Speech and Signal Processing, ICASSP'82*, vol. 3. Paris, France, May 1982, pp. 1325–1328.

[11] M. Pätzold, *Mobile Radio Channels*, 2nd ed. Chichester: John Wiley & Sons, 2011.

[12] M. Pätzold and B. Talha, "On the statistical properties of sum-of-cisoids-based mobile radio channel simulators," in *Proc. 10th International Symposium on Wireless Personal Multimedia Communications, WPMC 2007*. Jaipur, India, Dec. 2007, pp. 394–400.

[13] I. S. Gradshteyn and I. M. Ryzhik, *Table of Integrals, Series, and Products*, 7th ed. Elsevier Academic Press, 2007.

[14] R. H. Clarke, "A statistical theory of mobile-radio reception," *Bell Syst. Tech. Journal*, vol. 47, pp. 957–1000, Jul./Aug. 1968.

[15] M. Pätzold, B. O. Hogstad, and N. Youssef, "Modeling, analysis, and simulation of MIMO mobile-to-mobile fading channels," *IEEE Trans. Wireless Commun.*, vol. 7, no. 2, pp. 510–520, Feb. 2008.